Magnetic Properties

Access to Heteroleptic Fluorido-Cyanido Complexes with a Large Magnetic Anisotropy by Fluoride Abstraction

Jun-Liang Liu, Kasper S. Pedersen, Samuel M. Greer, Itziar Oyarzabal, Abhishake Mondal, Stephen Hill,* Fabrice Wilhelm, Andrei Rogalev, Alain Tressaud, Etienne Durand, Jeffrey R. Long, and Rodolphe Clérac*

Abstract: *Silicon-mediated fluoride abstraction is demonstrated as a means of generating the first fluorido-cyanido transition metal complexes. This new synthetic approach is exemplified by the synthesis and characterization of the heteroleptic complexes, trans-$[M^{IV}F_4(CN)_2]^{2-}$ (M = Re, Os), obtained from their homoleptic $[M^{IV}F_6]^{2-}$ parents. As shown by combined high-field electron paramagnetic resonance spectroscopy and magnetization measurements, the partial substitution of fluoride by cyanide ligands leads to a marked increase in the magnetic anisotropy of trans-$[ReF_4(CN)_2]^{2-}$ as compared to $[ReF_6]^{2-}$, reflecting the severe departure from an ideal octahedral (O_h point group) ligand field. This methodology paves the way toward the realization of new heteroleptic transition metal complexes that may be used as highly anisotropic building-blocks for the design of high-performance molecule-based magnetic materials.*

The fundamental coordination chemistry of 4d and 5d transition metal ions remains much less explored and developed than that of the lighter 3d congeners. However, recent results showing the promise of heavier transition metal ions in advanced inorganic and molecule-based materials have sparked interest in engineering their physical properties, notably their magnetic anisotropy.[1] Potential applications of these materials are intimately connected to the electronic structure of the metal ion, which, in turn, is determined by the nature of its coordination environment. The number of homo- and heteroleptic complexes of paramagnetic 4d and 5d ions remains low,[1, 2] reflecting the synthetic complications caused by the common robustness of the complexes of heavier transition metals. Indeed, only a few approaches exist to deliberately modify the coordination environment of such metal ions. Prominent examples of the 5d series include Re^{IV} and Os^{IV} metal ions, which, for instance, are found in both $[MF_6]^{2-}$ and $[M(CN)_7]^{3-}$ species.[3, 4] These two types of complexes differ not only in coordination geometry, but also in electronic structure, due to the entirely different nature of the perturbation imposed by cyanide and fluoride to the 5d orbitals, in accord with the spectrochemical series. Combining the two ligand types in a single 5d complex would provide an intriguing possibility of substantially altering their ligand field and, thus, their magnetic anisotropy.

Following this idea, we herein present the first examples of heteroleptic fluorido-cyanido complexes of any metal ion, as synthesized by a partial abstraction of coordinated fluoride ions.[5] This work was inspired by the recent isolation of

[*] Dr. J.-L. Liu, Prof. Dr. K. S. Pedersen, Dr. I. Oyarzabal, Dr. A. Mondal, Dr. R. Clérac
Univ. Bordeaux, CNRS, Centre de Recherche Paul Pascal, CRPP, UMR 5031, 33600 Pessac (France)
E-mail: clerac@crpp-bordeaux.cnrs.fr

Dr. I. Oyarzabal
Chemistry Faculty, University of the Basque Country UPV/EHU 20018 Donostia-San Sebastián (Spain)

Prof. Dr. S. Hill
Department of Physics, Florida State University
and
National High Magnetic Field Laboratory, Florida State University
Tallahassee, FL 32306 (USA)
E-mail: shill@magnet.fsu.edu

Dr. A. Tressaud, E. Durand
CNRS, ICMCB, UPR 9048, Univ. Bordeaux, 33608 Pessac (France)

Prof. Dr. J. R. Long
Department of Chemistry, University of California Berkeley (USA)
and
Department of Chemical and Biomolecular Engineering, University of California Berkeley (USA)
and
Materials Sciences Division, Lawrence Berkeley National Laboratory
Berkeley, CA 94720 (USA)

Dr. F. Wilhelm, Dr. A. Rogalev
ESRF-The European Synchrotron, 38043 Grenoble Cedex 9 (France)

Dr. J.-L. Liu
Current address: Key Laboratory of Bioinorganic and Synthetic Chemistry of Ministry of Education, School of Chemistry, Sun Yat-Sen University, Guangzhou 510275 (P. R. China)

Prof. Dr. K. S. Pedersen
Current address: Department of Chemistry, Technical University of Denmark, 2800, Kgs. Lyngby (Denmark)

Dr. A. Mondal
Current address: Solid State and Structural Chemistry Unit, Indian Institute of Science
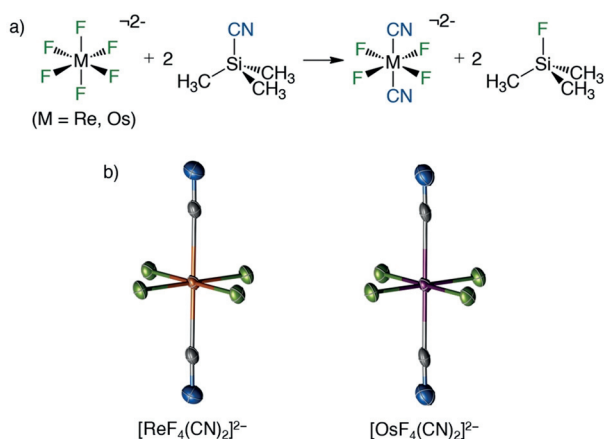C.V. Raman Road, Bangalore-560012 (India)

Dr. S. M. Greer
Department of Chemistry, Florida State University
and
National High Magnetic Field Laboratory, Florida State University
Tallahassee, FL 32306 (USA)
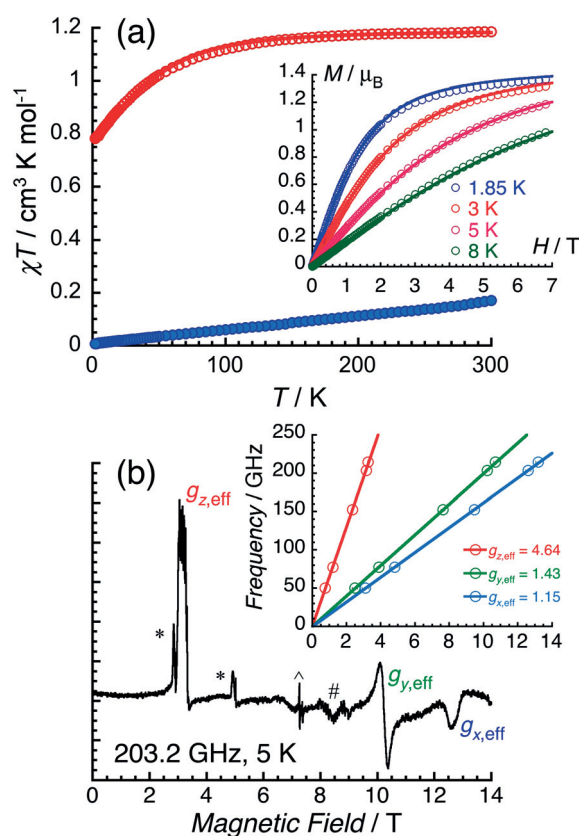
© 2020 Wiley-VCH Verlag GmbH & Co. KGaA, Weinheim

heteroleptic fluorido-cyanido anions of main-group elements, which were realized through fluoride abstraction from $[PF_6]^-$ using highly fluorophilic organo-silicon reagents.[6] For example, *cis*-$[PF_2(CN)_4]^-$ was isolated by the reaction of $[PF_6]^-$ with $(CH_3)_3SiCN$ under autogenous pressure at elevated temperatures.[6a] The driving force for this type of reaction is the difference in bond energy between the strong Si−F bond and the significantly weaker Si−C one (ΔH_f^{298K} (Si−F) = 540 kJ mol^{-1} vs. ΔH_f^{298K} (Si−C) = 435 kJ mol^{-1}).[7] To our knowledge, similar chemical reactivity in transition metal chemistry has never been reported.

The reaction of $(PPh_4)_2[MF_6]$ (M = Re, Os) with eight equivalents of $(CH_3)_3SiCN$ in dry CH_2Cl_2 at room-temperature and ambient pressure affords a single isolatable product of $(PPh_4)_2[$*trans*$-MF_4(CN)_2]\cdot H_2O$ (M = Re (**1**), Os (**2**)) in high yield (Figure 1a; see the Supporting Information for details). Single-crystal X-ray diffraction structure analysis of **1** and **2** (Figure 1b and Supporting Information, Tables S1 and S2) reveals the presence of an elongated octahedral coordination geometry for the *trans*-$[MF_4(CN)_2]^{2-}$ complexes, with M–F and M−C bond distances of 1.93–1.95 Å and 2.12–2.14 Å, respectively. Fluorine elemental analyses corroborate the presence of four fluoride ligands per metal ion, which is further supported by the isotope patterns observed in electrospray mass spectra (Supporting Information, Figures S2 and S3).[8]

The magnetic properties of these two unique heteroleptic complexes were probed using static (dc) magnetic susceptibility measurements. For **1**, the magnetic susceptibility-temperature product, χT, remains nearly constant from room temperature down to approximately 100 K (1.18–1.12 cm^3 K mol^{-1}, see Figure 2a). Considering a pure $S = 3/2$ spin ground state for the Re^{IV} magnetic center, the average g-factor can be estimated from the room-temperature χT value to be 1.58. Upon further cooling from 100 K, χT drops steadily to reach 0.78 cm^3 K mol^{-1} at 1.85 K. Given the absence of any close contacts between the complexes in the unit cell, this

Figure 2. a) Temperature dependence of the χT product at 0.1 T for **1** (red) and **2** (blue). Inset: Field (*H*) dependence of the magnetization (*M*) below 8 K for **1**. The solid lines are the best fit of the data for **1**, as described in the main text. b) High-field electron paramagnetic resonance (HF-EPR) spectrum obtained on a powdered sample of **1** at 5 K and 203.2 GHz; the inset shows the field dependence of the resonances and the fits yielding the effective g-factors, as described in the main text. In addition to the spectral features originating from **1** (designated $g_{x,eff}$, $g_{y,eff}$, and $g_{z,eff}$), signals from molecular dioxygen (*), a common $g = 2$ impurity (^), as well as an unidentified contribution (#) are observed.

behavior indicates the presence of a large zero-field splitting of the $^4A_{2g}$ (O_h) ground state. For **2**, the magnetic measurements reveal a room temperature χT product of 0.17 cm^3 K mol^{-1}, which decreases close to linearly with decreasing temperature and vanishes at the lowest temperatures (0.0063 cm^3 K mol^{-1} at 1.85 K). This thermal behavior is expected for a $^3T_{1g}$ (O_h) term in the presence of strong spin-orbit coupling that energetically isolates a non-magnetic $J_{eff} = 0$ ground state, leaving only a temperature independent paramagnetic contribution.[3b]

A quantitative analysis of the magnetic data for **1** was undertaken using the following spin-Hamiltonian [Eq. (1)]:

$$\hat{\mathcal{H}} = D\left(\hat{S}_z^2 - \frac{1}{3}S(S+1)\right) + E\left(\hat{S}_x^2 - \hat{S}_y^2\right)$$
$$+ \mu_B\left(g_x\hat{S}_xH_x + g_y\hat{S}_yH_y + g_z\hat{S}_zH_z\right)$$

$$(1)$$

This Hamiltonian contains five free variables including the zero-field splitting (ZFS) parameters D and E, and the three components of the g-tensor: g_x, g_y, and g_z. The relatively

Figure 1. a) Synthesis of *trans*-$[MF_4(CN)_2]^{2-}$ from the reaction of $[MF_6]^{2-}$ (M = Re, Os) with $(CH_3)_3SiCN$; b) View of the *trans*-$[MF_4(CN)_2]^{2-}$ molecular structure in **1** and **2** from their X-ray crystal structure with thermal ellipsoids drawn at the 50% probability level (Re orange, Os purple, F green, N blue, C grey). Selected bond lengths (Å) for **1**: Re−F 1.936(1), 1.951(1); Re−C 2.135(2); C−N 1.140(3), and for **2**: Os−F 1.926(1), 1.937(1); Os−C 2.115(3); C−N 1.086(3).[18]

featureless χT versus T and field-dependent magnetization plots (Figure 2a) do not provide sufficient constraints on the five parameters in Equation (1). To mitigate this problem, high-field electron paramagnetic resonance (HF-EPR) spectra of polycrystalline **1** were collected in magnetic fields up to 14 T, with multiple frequencies between 50 and 214 GHz (Figure 2b). Due to the sizable ZFS, only transitions between the components of the lower-lying Kramers doublet are observed. Hence, the $S = 3/2$ Re^{IV} center can be treated as an effective spin-1/2 ion with g_{eff}-values: $g_{z,eff} = 4.64$, $g_{y,eff} = 1.43$, and $g_{x,eff} = 1.15$ (inset of Figure 2b). In order to avoid over-parameterization, the three effective g-factors obtained from the HF-EPR data (Figure 2b) were first related to the $\gamma = E/D$ ratio and the eigen-values of the actual $S = 3/2$ g-tensor (see the Supporting Information).[9] Subsequently, the average of the Cartesian components of this g-tensor,

$$g_{average} = \sqrt{(g_x^2 + g_y^2 + g_z^2)/3},$$ was fixed to the powder-averaged g-factor extracted from the static magnetic susceptibility at high temperature: $g = 1.58$ at 270 K, which leads to only eight possible γ values (Supporting Information, Figure S7). However, six of them can be excluded as they result in physically unreasonable g-values ($g_i > 2$ or $g_i \leq 1$) for a system with a less than half-filled d-shell exhibiting a quenched first-order orbital angular momentum. The two remaining solutions are characterized by $D < 0$, $E/D = \pm 0.328$, and the following g-tensor components: $g_{x(y)} = 1.45$, $g_{y(x)} = 1.59$, and $g_z = 1.69$. Indeed, these two solutions are identical as they are simply related by a permutation of the x and y axes, corresponding to a change in the sign of E (Supporting Information, Table S3).

Using the above set of initial parameters, the magnetic and spectroscopic data were simultaneously fit without any further constraints, yielding the parameters: $D/k_B = -69.5$ K (-48.3 cm^{-1}), $|E|/k_B = 22.6$ K (15.7 cm^{-1}), $g_{x(y)} = 1.46$, $g_{y(x)} = 1.60$, and $g_z = 1.69$. The best-fit results are shown in Figure 2, and the calculated effective g-values ($g_{z,eff(calc)} = 4.64$, $g_{y,eff(calc)} = 1.43$, $g_{x,eff(calc)} = 1.15$) are in perfect agreement with the HF-EPR data. The large values of the ZFS parameters, D and E, give rise to a large energy gap, $\Delta/k_B = \left(2\sqrt{D^2 + 3E^2}\right)/k_B = 160$ K (111 cm^{-1}), between the two doublets of the $S = 3/2$ state. These experimentally observed ZFS parameters are reasonably well reproduced by CASSCF/NEVPT2 calculations, which, using the effective Hamiltonian approach, predict $D/k_B = -91.0$ K (-63.2 cm^{-1}) and $E/D = 0.21$ (Supporting Information, Figure S8 and Tables S4 and S5).[10] Remarkably, the obtained energy gap is much larger than that found for the parent [ReF$_6$]$^{2-}$ complex ($\Delta/k_B = 69$ K)[3a] and the structurally related trans-[ReCl$_4$(CN)$_2$]$^{2-}$ complex ($\Delta/k_B = 35$ K).[11]

The electronic structure of **1** was further studied by X-ray absorption (XAS) and X-ray magnetic circular dichroism (XMCD) spectroscopy at the L_3 (2p$_{3/2}$→5d$_{3/2,5/2}$) and L_2 (2p$_{1/2}$→5d$_{3/2}$) absorption edges of rhenium at 3 K in magnetic fields up to 17 T. As expected, the XAS spectrum (Figure 3) shows intense resonant absorption ("white lines") at both edges. Their integrals are related to the $\langle \Sigma_i \mathbf{l}_i \cdot \mathbf{s}_i \rangle$ expectation value, summed over all 5d electrons, through the spin-orbit
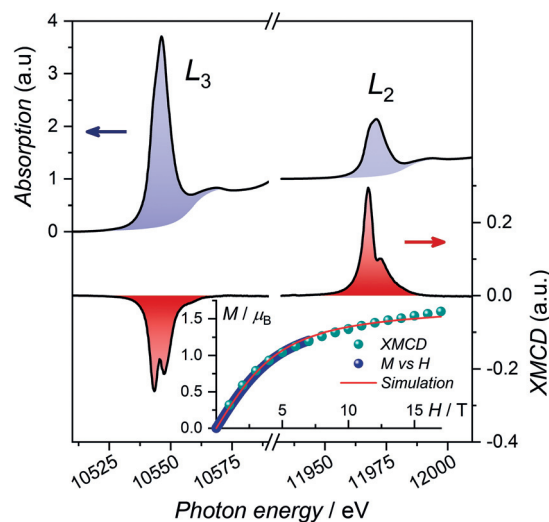

Figure 3. Isotropic XAS (top) and XMCD (bottom) spectra of a powdered sample of **1** obtained at the L_3 and L_2 rhenium absorption edges in magnetic fields of ±17 T at 3 K. The inset shows the field dependence of the maximum dichroism signal intensity at the rhenium L_2 edge scaled to the M vs. H data obtained by magnetization measurements.

sum rule, which amounts to $\langle \Sigma_i \mathbf{l}_i \cdot \mathbf{s}_i \rangle/\hbar^2 = -1.56$ in **1** (see the Supporting Information),[12] in perfect agreement with the reported value (-1.6) for the isoelectronic Os^V in [Os^{V}F$_6$]$^-$.[3b] The XMCD spectra were recorded as the difference between two subsequent XAS spectra obtained with right and left circularly polarized X-rays and under magnetic field applied either parallel or antiparallel to the X-ray wavevector. At both the L_2 and L_3 edges, strong XMCD signals with opposite signs are observed (Figure 3). The scaling of the field-dependent XMCD signal intensity at the L_2 edge to the field dependence of the powder magnetization data at 3 K allows an estimation of the absolute value of the magnetization at 17 T (Figure 3, inset) as 1.6 μ_B. Through the magneto-optical sum rules,[13] the orbital and spin magnetic moments of the rhenium 5d states could be separately determined to be $M_{orbital} = -\langle L_z \rangle \mu_B = 0.01 \mu_B$ and $M_{spin} = 1.6 \mu_B$, following the previously reported approach (see the Supporting Information).[14] These numbers reflect the virtual total quenching of the orbital angular momentum by the ligand field which, in turn, provides the basis for neglecting orbitally dependent terms in Equation (1).

In order to probe the magnetization dynamics of **1**, alternating-current (ac) magnetic susceptibility measurements were performed. In contrast to zero-dc field, slow relaxation of the magnetization for **1** is clearly observed in the available experimental window in the presence of a static magnetic field (Figure 4 and Supporting Information, Figure S4). The field and temperature dependence of the relaxation time, τ, were estimated by fitting the $\chi'(\nu)$ and $\chi''(\nu)$ data to the generalized Debye model and their associated standard deviation was calculated from the obtained α parameter (Figure 5 and Supporting Information, Figures S5 and S6).[15] As shown in Figure 5, the estimated standard deviation of τ is large and, thus, the following analysis of the relaxation must be taken with a certain
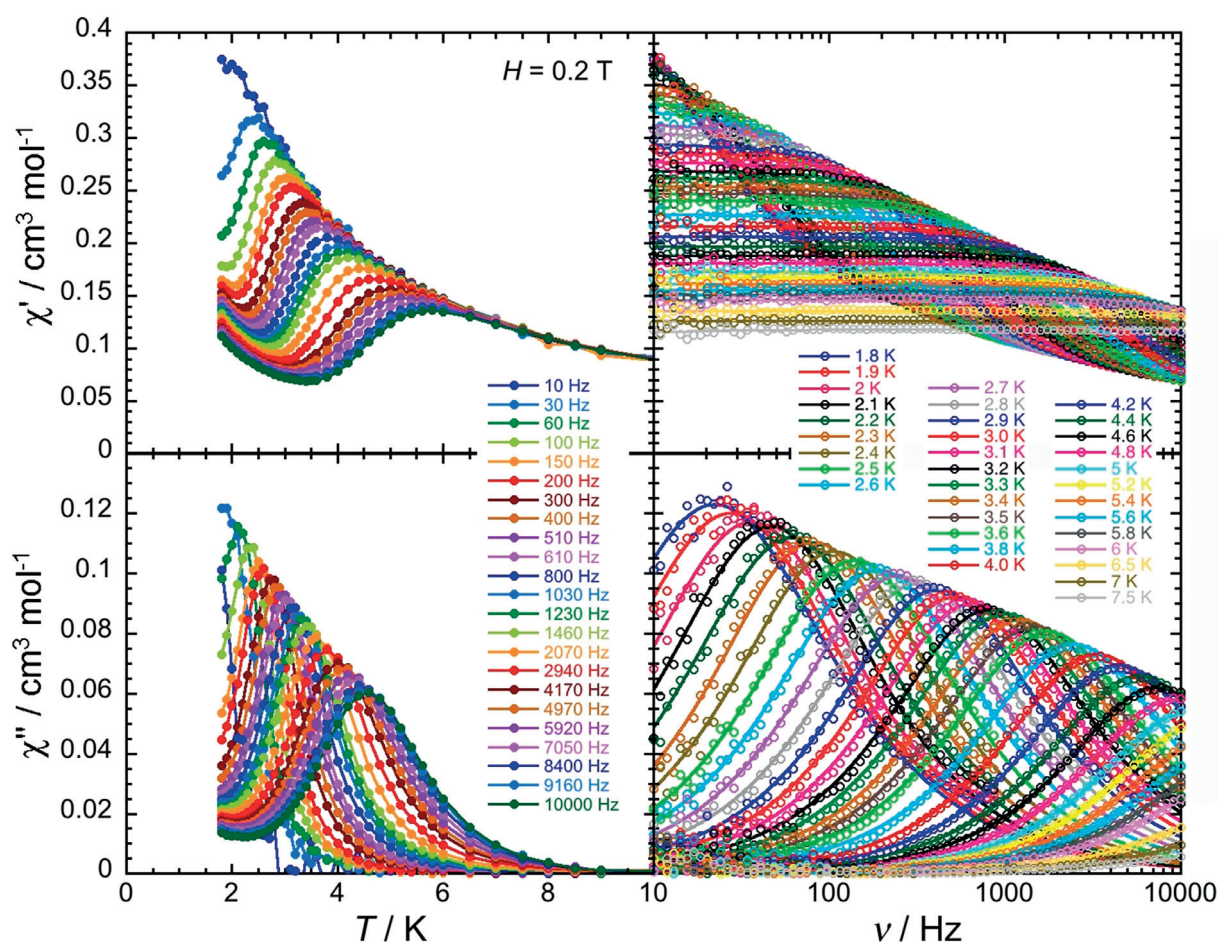
Figure 4. Temperature (left) and ac frequency (right) dependences of the real (χ', top) and imaginary (χ'', bottom) parts of the ac susceptibility, between 1.85 and 10 K and between 10 and 10000 Hz, for **1** in a 0.2-T dc field. Solid lines are visual guides on the left plots while they show the generalized Debye fits of the ac susceptibility data on the right.
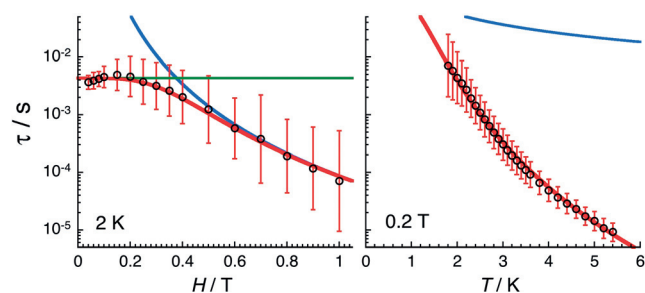
Figure 5. Field (left) and temperature (right) dependences of the relaxation time, τ, for **1** estimated from the generalized Debye fits of the ac susceptibility data shown in Figure S4 in the Supporting Information and Figure 4 collected at 2 K and under a 0.2-T applied field, respectively. The estimated standard deviation of the relaxation time (vertical red bars) were calculated from the average α parameter of the generalized Debye fit (Supporting Information, Figures S5 and S6) and a log-normal distribution as described in ref. [15]. The red line is the best fit including Raman (green line) and direct (blue line) relaxation processes, as discussed in the text.

caution. Considering the field dependence at 2 K (Figure 5, left), two regimes are clearly observed: i) below 0.2 T, the relaxation time is quasi-field-independent indicating the absence of a significant magnetization relaxation via quantum

tunneling; meanwhile, ii) above 0.2 T, τ decreases following an H^{-4} variation as expected in the case of a one-phonon direct process $(\tau_{\text{direct}}(H,T)^{-1} = AH^4T)$.[16,17] The temperature dependence of the relaxation time shown in Figure 5 and Figure S6 in the Supporting Information is more difficult to analyze as the semilogarithmic τ vs. T^{-1} plot (Supporting Information, Figure S6) does not follow a simple Arrhenius behavior compatible with an Orbach mechanism. On the other hand, the τ vs. T data at 0.2 T are almost perfectly reproduced by a power law compatible with a Raman process which, to a first approximation, can be considered as magnetic field independent $(\tau_{\text{Raman}}(H,T)^{-1} = CT^n)$.[17] Therefore, the field and temperature dependence of the relaxation time were fitted simultaneously to a model including both direct and Raman processes $(\tau(H,T)^{-1} = \tau_{\text{direct}}(H,T)^{-1} + \tau_{\text{Raman}}(H,T)^{-1} = AH^4T + CT^n)$. As shown in Figure 5, the experimental τ vs. H (at 2 K) and τ vs. T (at 0.2 T) data are perfectly reproduced by this three-parameter model with $A = 5.7(3) \times 10^3 \text{ s}^{-1}\text{K}^{-1}\text{T}^{-4}$, $C = 2.9(3) \text{ s}^{-1}\text{K}^{-6.3}$ and $n = 6.3(1)$. These results suggest that the paramagnetic relaxation between 1.8 and 5.4 K is governed in **1** by direct and Raman processes only. Significantly, this conclusion is different from that reported for the related *trans*-[ReCl$_4$(CN)$_2$]$^{2-}$ complex, wherein the Orbach process $(\tau_0 = 5.7 \times 10^{-11} \text{ s}$, and $\Delta_{\text{eff}}/k_B =$

39 K) dominates over similar Raman and direct mechanisms ($A = 29 \times 10^3\ s^{-1}\ K^{-1}\ T^{-4}$, $C = 2.5\ s^{-1}\ K^{-6.9}$ and $n = 6.9$), likely due to the much smaller energy splitting between the two Kramers doublets (39 K) than for **1** (160 K).[11b]

In summary, the first two fluorido-cyanido transition metal complexes have been realized through silicon-mediated fluoride abstraction. The structural and magnetic properties of these heteroleptic complex salts, $(PPh_4)_2[trans\text{-}M^{IV}F_4(CN)_2]\cdot H_2O$ (M = Re and Os), have been studied in great detail. For the Re^{IV} compound, the combined analysis of high-field EPR and magnetization data circumvents the common problem of overparameterization of powder- and thermodynamically averaged magnetization data and provides an unambiguous determination of the zero-field splitting parameters and g-tensor. Notably, the measured magnetic anisotropy, reflected by the 160 K energy gap between the two doublets of the $S = 3/2$ ground state, is one of the largest known for a 5d transition metal complex,[2c,3a,11] which illustrates the viability of our synthetic methodology to target new heteroleptic transition metal complexes with strong magnetic anisotropy.

Conflict of interest

The authors declare no conflict of interest.

[1] X.-Y. Wang, C. Avendaño, K. R. Dunbar, *Chem. Soc. Rev.* **2011**, *40*, 3213–3238.

[2] a) M. P. Shores, J. J. Sokol, J. R. Long, *J. Am. Chem. Soc.* **2002**, *124*, 2279–2292; b) T. D. Harris, M. V. Bennett, R. Clérac, J. R. Long, *J. Am. Chem. Soc.* **2010**, *132*, 3980–3988; c) J. Martínez-Lillo, T. F. Mastropietro, E. Lhotel, C. Paulsen, J. Cano, G. De Munno, F. Faus, F. Lloret, M. Julve, S. Nellutla, J. Krzystek, *J. Am. Chem. Soc.* **2013**, *135*, 13737–13748; d) J. Martínez-Lillo, F. Faus, F. Lloret, M. Julve, *Coord. Chem. Rev.* **2015**, *289–290*, 215–217.

[3] a) K. S. Pedersen, M. Sigrist, M. A. Sørensen, A.-L. Barra, T. Weyhermüller, S. Piligkos, C. A. Thuesen, M. G. Vinum, H. Mutka, H. Weihe, R. Clérac, J. Bendix, *Angew. Chem. Int. Ed.* **2014**, *53*, 1351–1354; *Angew. Chem.* **2014**, *126*, 1375–1378; b) K. S. Pedersen, D. N. Woodruff, S. K. Singh, A. Tressaud, E. Durand, M. Atanasov, P. Perlepe, K. Ollefs, F. Wilhelm, C. Mathonière, F. Neese, A. Rogalev, J. Bendix, R. Clérac, *Chem. Eur. J.* **2017**, *23*, 11244–11248.

[4] a) M. V. Bennett, J. R. Long, *J. Am. Chem. Soc.* **2003**, *125*, 2394–2395; b) E. V. Peresypkina, A. Gavriluta, K. E. Vostrikova, *Crystals* **2016**, *6*, 102; c) D. E. Freedman, D. M. Jenkins, A. T. Iavarone, J. R. Long, *J. Am. Chem. Soc.* **2008**, *130*, 2884–2885; d) D. G. Samsonenko, C. Paulsen, E. Lhotel, V. S. Mironov, K. E. Vostrikova, *Inorg. Chem.* **2014**, *53*, 10217–10231.

[5] a) N. M. Doherty, N. W. Hoffman, *Chem. Rev.* **1991**, *91*, 553–573; b) J. L. Kiplinger, T. G. Richmond, C. E. Osterberg, *Chem. Rev.* **1994**, *94*, 373–431; c) E. F. Murphy, R. Murugavel, H. W. Roesky, *Chem. Rev.* **1997**, *97*, 3425–3468.

[6] a) J. Bresien, S. Ellinger, J. Harloff, A. Schulz, K. Sievert, A. Stoffers, C. Täschler, A. Villinger, C. Zur Täschler, *Angew. Chem. Int. Ed.* **2015**, *54*, 4474–4477; *Angew. Chem.* **2015**, *127*, 4556–4559; b) J. Harloff, D. Michalik, S. Nier, A. Schulz, P. Stoer, A. Villinger, *Angew. Chem. Int. Ed.* **2019**, *58*, 5452–5456; *Angew. Chem.* **2019**, *131*, 5506–5511.

[7] J. A. Dean in *Lange's Handbook of Chemistry*, 15th ed., McGraw-Hill, Inc., New York; London, **1999**, pp. 4.50.

[8] L. Patiny, A. Borel, *J. Chem. Inf. Model.* **2013**, *53*, 1223–1228.

[9] R. Boča in *A Handbook of Magnetochemical Formulae*, Elsevier, Oxford, **2012**, pp. 189–230; J. R. Pilbrow, *J. Magn. Reson.* **1978**, *31*, 479–490.

[10] F. Neese, *WIREs Comput. Mol. Sci.* **2018**, *8*, e1327.

[11] a) X. Feng, J. Liu, T. D. Harris, S. Hill, J. R. Long, *J. Am. Chem. Soc.* **2012**, *134*, 7521–7529; b) X. Feng, J.-L. Liu, K. S. Pedersen, J. Nehrkorn, A. Schnegg, K. Holldack, J. Bendix, M. Sigrist, H. Mutka, D. Samohvalov, D. Aguilà, M.-L. Tong, J. R. Long, R. Clérac, *Chem. Commun.* **2016**, *52*, 12905–12908.

[12] G. van der Laan, B. T. Thole, *Phys. Rev. Lett.* **1988**, *60*, 1977–1980.

[13] a) B. T. Thole, P. Carra, F. Sette, G. van der Laan, *Phys. Rev. Lett.* **1992**, *68*, 1943–1946; b) P. Carra, B. T. Thole, M. Altarelli, X. Wang, *Phys. Rev. Lett.* **1993**, *70*, 694–697.

[14] K. S. Pedersen, J. Bendix, A. Tressaud, E. Durand, H. Weihe, Z. Salman, T. J. Morsing, D. N. Woodruff, Y. Lan, W. Wernsdorfer, C. Mathonière, S. Piligkos, S. I. Klokishner, S. Ostrovsky, K. Ollefs, F. Wilhelm, A. Rogalev, R. Clérac, *Nat. Commun.* **2016**, *7*, 12195.

[15] D. Reta, N. F. Chilton, *Phys. Chem. Chem. Phys.* **2019**, *21*, 23567–23575.

[16] A. Abragam, B. Bleaney, *Electron Paramagnetic Resonance of Transition Ions*, Dover, New York, **1986**.

[17] K. N. Shrivastava, *Phys. Status Solidi A* **1983**, *117*, 437–458.

[18] CCDC 1531669 (**1**) and 1531670 (**2**) contain the supplementary crystallographic data for this paper. These data are provided free of charge by The Cambridge Crystallographic Data Centre.